



This is a repository copy of *Black holes, TeV-scale gravity and the LHC*.

White Rose Research Online URL for this paper:

<https://eprints.whiterose.ac.uk/98094/>

Version: Accepted Version

Proceedings Paper:

Winstanley, E. orcid.org/0000-0001-8964-8142 (2013) Black holes, TeV-scale gravity and the LHC. In: Proceedings of the Time & Matter conference 2013. Time and Matter 2013, 04-08 Mar 2013, Venice, Italy. .

Reuse

Items deposited in White Rose Research Online are protected by copyright, with all rights reserved unless indicated otherwise. They may be downloaded and/or printed for private study, or other acts as permitted by national copyright laws. The publisher or other rights holders may allow further reproduction and re-use of the full text version. This is indicated by the licence information on the White Rose Research Online record for the item.

Takedown

If you consider content in White Rose Research Online to be in breach of UK law, please notify us by emailing eprints@whiterose.ac.uk including the URL of the record and the reason for the withdrawal request.



eprints@whiterose.ac.uk
<https://eprints.whiterose.ac.uk/>

Black holes, TeV-scale gravity and the LHC

ELIZABETH WINSTANLEY *

*Consortium for Fundamental Physics, The University of Sheffield,
Hicks Building, Hounsfield Road, Sheffield. S3 7RH United Kingdom*

Abstract: Over the past 15 years models with large extra space-time dimensions have been extensively studied. We have learned from these models that the energy scale of quantum gravity may be many orders of magnitude smaller than the conventional value of 10^{19} GeV. This raises the tantalizing prospect of probing quantum gravity effects at the LHC. Of the possible quantum gravity processes at the LHC, the formation and subsequent evaporation of microscopic black holes is one of the most spectacular. We give an overview of some of the fundamental ideas of the large extra dimensions scenarios and the resulting black hole processes at the LHC.

Introduction

The possibility of producing microscopic black holes at the Large Hadron Collider (LHC) is one of the most exciting consequences of “brane world” models developed over the past 15 years or so. The purpose of this presentation is to outline the theories behind this intriguing possibility: gravitational theories in which the energy scale of quantum gravity is much lower than the conventional value of 10^{19} GeV, and may possibly be as low as a few TeV. We will also describe some of the features of black hole creation and evolution in these low-scale quantum gravity theories. Finally we link the theoretical modelling to experimental searches for black holes at the LHC.

There is a vast literature on this subject and in this brief note we cannot do more than outline a few aspects. We have not aimed to be complete in our coverage of the subject, nor in the references. The reader is encouraged to consult the many reviews [1, 2] for further details.

* E.Winstanley@sheffield.ac.uk

Large extra dimensions

Einstein's theory of general relativity can be formulated in any number of space-time dimensions, although all observations to date agree that we live in a Universe with three space and one time dimension. Gravitational theories in more than four space-time dimensions have been studied for many years (beginning with Kaluza-Klein theory in the 1920s). These extra dimensions have proved invisible to observations because their size is smaller than any observable length scale. For example, in conventional superstring theory, the extra dimensions are assumed to be compactified and to have size roughly the order of the Planck length L_P , the natural length scale in quantum gravity:

$$L_P = \sqrt{\frac{\hbar G}{c^3}} \sim 10^{-35} \text{ m.} \quad (1)$$

Our focus in this note are higher-dimensional theories with large extra dimensions, where "large" means "large compared with the Planck length" (1). Such theories have been developed as a possible resolution of the hierarchy problem. The hierarchy problem asks why the natural energy scale of quantum gravity, the Planck energy E_P

$$E_P = \sqrt{\frac{\hbar c^5}{G}} \sim 10^{19} \text{ GeV,} \quad (2)$$

is so much bigger (about 17 orders of magnitude) than the natural energy scales of the other fundamental forces in nature (for example, the electroweak scale is about 100 GeV). We restrict our attention to one model with large extra dimensions, the ADD scenario [3].

In the ADD model, there are n extra dimensions which are compactified on a length scale R . A comparatively large volume for these extra compact dimensions lowers the fundamental, higher-dimensional scale of quantum gravity to $E_* \ll E_P$. By integrating out the n extra dimensions, the effective scale of quantum gravity observed in four dimensions, E_P (2), is related to E_* by

$$E_P^2 \sim R^n E_*^{2+n}. \quad (3)$$

By making the size of the extra dimensions sufficiently large, the energy scale E_* can be made many orders of magnitude smaller than E_P . For example, for $n = 5$ extra dimensions and $R \sim 10^{-13}$ m, we have $E_* \sim 1$ TeV, within the LHC energy range.

While length scales of this size have not been probed gravitationally, they have been probed using particle physics experiments. In order to

avoid a contradiction with the Standard Model of Particle Physics, the higher-dimensional space-time in the ADD scenario is comprised of a four-dimensional brane which is embedded into a higher-dimensional bulk space-time. All Standard Model particles and forces are confined to the brane, and only gravitational degrees of freedom can propagate in the bulk. The effective energy scale for quantum gravity on the brane is E_P (2), while the higher-dimensional energy scale for quantum gravity in the bulk is E_* (3). Models such as the ADD scenario are known as “brane-world” models.

Theories with large extra dimensions and low-scale quantum gravity, such as the ADD scenario outlined above, have many interesting consequences. For example, a collider experiment with centre-of-mass energy $\sqrt{s} > E_*$ will probe the strong gravity regime. This raises the exciting possibility that quantum gravity effects may not be many orders of magnitude out of the reach of terrestrial experiments, but may be probed at the LHC. In this note we are concerned with one of the most spectacular strong gravity processes, namely the production of black holes in high-energy collisions [4, 5, 6].

Production of microscopic black holes

The basic idea behind the production of black holes in high-energy particle collisions is very simple. Consider two colliding particles whose combined centre-of-mass energy is somewhat larger than E_* . In four space-time dimensions, Thorne’s “Hoop Conjecture” [7] states that a black hole will form if the energy of the particles is compressed into a region whose circumference in every direction is less than $2\pi r_H$, where r_H is the radius of a Schwarzschild black hole having energy equal to the total energy of the particles. In more than four space-time dimensions, the “Hoop Conjecture” is modified slightly [8], but the fundamental principle is the same: if the energy of the colliding particles is squeezed into a small enough region, then a black hole is expected to form.

For the moment, let us consider the formation of a black hole as a purely classical process, described by general relativity. Consider two colliding particles (modelling the partons inside the protons at the LHC), their distance of closest approach being the impact parameter b (see Figure 1). The quantity of prime importance for collider physics is the parton-level production cross-section σ , which is required for simulating full production cross-sections for experimental searches. The parton-level production cross-section is related to the maximum impact parameter b_{max} for which

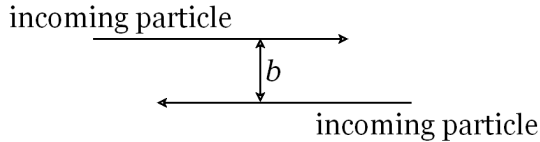


Figure 1: Two colliding particles with impact parameter b .

a black hole forms from the colliding particles by the geometric formula

$$\sigma = \pi b_{max}^2. \quad (4)$$

There are two main approaches to studying these collisions and hence finding b_{max} .

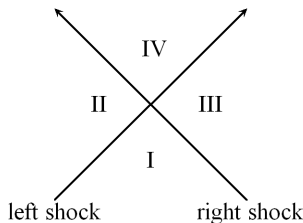


Figure 2: The collision of two Aichelburg-Sexl shock waves.

The first models the colliding particles as two gravitational shock waves [9], which are infinitely boosted black holes (see Figure 2). The formation of a closed trapped surface in the future of the collision of the two gravitational shock waves (region IV in Figure 2) indicates that a black hole has formed. The advantage of this approach is that the metric for each gravitational shock wave is known analytically. The two shock wave metrics can be superimposed in regions I-III in Figure 2 because, by causality, they can only affect each other in region IV. The equation defining a closed trapped surface in region IV has, in general, to be solved numerically. In four space-time dimensions, for non-zero impact parameter b , this approach was pioneered by Eardley and Giddings [10] building on unpublished work of Penrose and four-dimensional work of D'Eath and Payne for the $b = 0$ case [11]. Subsequently higher-dimensional collisions have also been investigated [12, 13].

In the second approach, the colliding particles are modelled as boson stars, fluid particles or black holes and the space-time which evolves as the

two objects collide is computed using full numerical relativity. Over the past eight or so years, numerical relativity has made enormous advances, which have allowed ultra-relativistic collisions between high-velocity objects to be studied. To date, most attention has focussed on collisions in four space-time dimensions [14]. Higher-dimensional work is, comparatively, in its infancy (see [15] for some recent reviews).

In both of the above approaches, the maximum impact parameter b_{max} is found to be a numerical factor times r_H , the event horizon radius of a black hole having the same energy as the combined energy of the colliding particles. The maximum impact parameter b_{max} then gives the parton-level geometric production cross-section σ (4). Some example values of σ are given in Table 1 [12].

n	0	1	2	3	4	5	6	7
$\sigma / (\pi r_H^2)$	0.71	1.54	2.15	2.52	2.77	2.95	3.09	3.20

Table 1: Parton-level black hole production cross-sections σ for various numbers of space-time dimensions $D = 4 + n$ [12].

The parton-level black hole production cross-sections then feed into the full production cross-sections [5, 6]. There are many parameters involved in estimating these cross-sections (for example, the value of E_* and the number of space-time dimensions). Depending on the the values of these parameters, it is possible to construct very optimistic cross-sections; for example, with $E_* = 1$ TeV and $n = 6$ extra dimensions, the production cross-section for black holes with a mass of $5 \text{ TeV}/c^2$ is about one black hole per second (that is, about 10^5 fb)! However, the cross-section decreases very rapidly as the black hole mass (or E_*) increases; for example, keeping $E_* = 1$ TeV and $n = 6$ extra dimensions, the cross-section for black holes with a mass of $10 \text{ TeV}/c^2$ is about 10 fb (which is still significant).

We emphasize that the production of black holes at the LHC is only a realistic possibility for higher-dimensional models outlined in the previous section, in which the fundamental energy scale of quantum gravity is about $10^0 - 10^1$ TeV. Any black holes which form will be microscopic in scale, having radii about $\sim 10^{-4}$ fm.

Microscopic black hole decay

We now consider what happens to a microscopic black hole formed by particle collisions at the LHC. When initially created, the black hole will be highly asymmetric and will have attached gauge field hair arising from

the gauge field quantum numbers of the colliding partons. The black hole will also be rapidly rotating, due to the initial angular momentum in the configuration shown in Figure 1. We assume that the initial energy of the black hole is at least a few times greater than the quantum gravity scale E_* , so that its geometry can be described in terms of general relativity (see [16] for more on this assumption). This is the semi-classical approximation - we consider quantum processes on the classical black hole background.

The subsequent evolution of the black hole can be described in terms of four stages [6]:

Balding phase The black hole sheds its asymmetries and attached gauge field hair. This phase is often modelled as part of the black hole production process. At the end of this phase the black hole is still rapidly rotating.

Spin-down phase The black hole emits Hawking radiation, losing mass and angular momentum. At the end of this phase the black hole is not rotating.

Schwarzschild phase The black hole is now spherically symmetric and continues to emit Hawking radiation.

Planck phase When the energy of the black hole is of the same order as the quantum gravity scale E_* , its geometry can no longer be described by general relativity and the full details of quantum gravity effects (which are ignored in the semi-classical approximation) become important.

We now briefly discuss each of these phases.

Balding phase

One of the key questions concerning the balding phase is how much of the initial energy of the colliding particles is shed in gravitational radiation as the black hole forms. Both the colliding shock wave model and full numerical relativity calculations outlined above give upper bounds on this and therefore lower bounds on the mass of the black hole. For example, for head-on colliding shock waves, the energy of the black hole is at least 70% of the initial energy for collisions in four space-time dimensions, and at least 58% of the initial energy for collisions in eleven space-time dimensions [10]. As an example of the results from numerical relativity, four-dimensional calculations indicate that about 50% of the initial energy of the colliding particles is radiated away in the ultra-relativistic limit [17].

The emitted gravitational radiation has also been studied by a number of other approaches - see the reviews [1, 2] for fuller discussions.

The second aspect of the balding phase is the shedding of charges and gauge field hair. This has not received much attention in the literature. In particular, QCD effects are likely to be very important at the LHC, but there is little work on this [18]. The effect of electric charge on the formation process has been studied in numerical relativity [19], and upper bounds on the amount of electromagnetic as well as gravitational radiation have been computed.

Naively one would expect that any electric charge left on the black hole would rapidly discharge due to Schwinger pair production. However, this assumption is based on conventional four-dimensional gravity models where electromagnetic interactions are many orders of magnitude stronger than gravitational interactions. In higher-dimensional gravity models with strong gravity, the loss of electric charge is not so rapid [20].

Black hole at the end of the balding phase

At the end of the balding phase, the higher-dimensional black hole that remains is uncharged, axisymmetric and rapidly rotating. The space of solutions of general relativity describing rotating black objects in more than four space-time dimensions is extremely rich [21] (see [22] for discussions of black holes in brane world models). Here we employ a very simple model of the black hole. Working in the ADD scenario, we assume that the extra dimensions are flat and that the black hole is very much smaller than the compactification radius of the extra dimensions (so that the compactification can effectively be ignored). We also assume that the brane has no tension or energy density.

In higher-dimensional vacuum general relativity, the generalization of the four-dimensional Kerr geometry describing a rotating black hole is the Myers-Perry family of metrics [23]. For black holes created by particle collisions on the brane, we are interested in black holes which have a single axis of rotation, lying in the brane. In this case the Myers-Perry metric takes the form

$$\begin{aligned}
 ds^2 = & \left(1 - \frac{\mu}{\Sigma r^{n-1}}\right) dt^2 + \frac{2a\mu \sin^2 \theta}{\Sigma r^{n-1}} dt d\varphi - \frac{\Sigma}{\Delta_n} dr^2 - \Sigma d\theta^2 \\
 & - \left(r^2 + a^2 + \frac{a^2 \mu \sin^2 \theta}{\Sigma r^{n-1}}\right) \sin^2 \theta d\varphi^2 - r^2 \cos^2 \theta d\Omega_n^2
 \end{aligned} \quad (5)$$

where

$$\Delta_n = r^2 + a^2 - \frac{\mu}{r^{n-1}}, \quad \Sigma = r^2 + a^2 \cos^2 \theta. \quad (6)$$

The parameters μ and a determine the mass M and angular momentum J of the black hole:

$$M = \frac{(n+2) A_{n+2} \mu}{16\pi G_{4+n}}, \quad J = \frac{2aM}{n+2} \quad (7)$$

where n is the number of extra dimensions, A_{n+2} is the surface area of an $(n+2)$ -dimensional unit sphere and G_{4+n} is the higher-dimensional Newton constant. The black hole has an event horizon at $r = r_H$, which is the largest positive root of the equation $\Delta_n = 0$. The event horizon rotates with an angular velocity

$$\Omega_H = \frac{a}{r_H^2 + a^2}. \quad (8)$$

We emphasize that the metric (5) is a solution of the $(n+4)$ -dimensional vacuum Einstein equations.

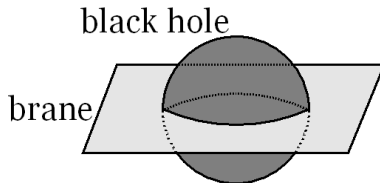


Figure 3: The geometry of a higher-dimensional black hole on the brane.

In the ADD model, the higher-dimensional black hole will lie on the brane (on which the Standard Model particles and forces are confined), as shown in Figure 3. In the full Myers-Perry metric (5), the co-ordinates (t, r, θ, φ) are the co-ordinates on the brane and $d\Omega_n^2$ is the part of the metric coming from the extra dimensions. Fixing the co-ordinates in the extra dimensions, the metric on the brane “slice” of the Myers-Perry black hole takes the form:

$$ds^2 = \left(1 - \frac{\mu}{\Sigma r^{n-1}}\right) dt^2 + \frac{2a\mu \sin^2 \theta}{\Sigma r^{n-1}} dt d\varphi - \frac{\Sigma}{\Delta_n} dr^2 - \Sigma d\theta^2 - \left(r^2 + a^2 + \frac{a^2 \mu \sin^2 \theta}{\Sigma r^{n-1}}\right) \sin^2 \theta d\varphi^2. \quad (9)$$

This is the four-dimensional black hole metric seen by observers on the brane. Note that the metric (9) still depends on the number of extra dimensions n . For $n = 0$ it reduces to the usual Kerr metric. However, for $n > 0$ the metric (9) is not a solution of the vacuum Einstein equations in four space-time dimensions [20].

Spin-down and Schwarzschild phases

During these two phases of the black hole evolution, the black hole metric is assumed to be classical. The black hole will emit quantum thermal Hawking radiation [24], with a temperature given by

$$T_H = \frac{(n+1)r_H^2 + (n-1)a^2}{4\pi(r_H^2 + a^2)r_H} \quad (10)$$

for the Myers-Perry black hole (5) (the temperature is the same on the brane and in the bulk space-time). The semi-classical approximation remains valid as long as the energy of each emitted quantum is a small proportion of the energy of the black hole. This remains true until the energy of the black hole is close to the energy scale of quantum gravity E_* , when the Planck regime is reached.

In the ADD scenario, Standard Model particles (fermions, gauge bosons and Higgs) can only be emitted on the brane. In contrast, gravitons (and possibly some scalars associated with gravitational degrees of freedom) can be emitted both on the brane and in the bulk. While the gravitational radiation in the bulk cannot be observed, it contributes to the missing energy in black hole events.

The Hawking radiation for each species is computed by starting with the classical field equations on the bulk black hole background (5) or brane black hole background (9) as appropriate. For four-dimensional Kerr black holes, Teukolsky [25] developed a formalism which writes the equations for fields of spin 0 (scalars), $\frac{1}{2}$ (fermions), 1 (gauge bosons) and 2 (gravitons) in terms of a single ‘‘master’’ equation for a quantity Ψ (the exact nature of Ψ depending on the spin of the field). Teukolsky’s formalism can be extended to fields of spin 0, $\frac{1}{2}$ and 1 (that is, the fields of the Standard Model) on the brane metric (9) (see [2, 26] for more details). The field quantity Ψ is then expanded in terms of modes of frequency ω :

$$\Psi = \sum_{\omega\ell m} R_{s\omega\ell m}(r) S_{s\omega\ell m}(\theta) e^{-i\omega t} e^{im\varphi}, \quad (11)$$

where s is the spin of the field, ℓ the total angular momentum quantum number and m the azimuthal quantum number. The angular function $S_{s\omega\ell m}(\theta)$ is a spin-weighted spheroidal harmonic, and the radial function $R_{s\omega\ell m}(r)$ can only be computed numerically.

To study the Hawking radiation, we are interested in ‘‘up’’ modes for which the radial function takes the typical form

$$R_{s\omega\ell m} = \begin{cases} e^{i\tilde{\omega}r_*} + A_{\omega\ell m}^{\text{up}} e^{-i\tilde{\omega}r_*}, & r_* \rightarrow -\infty, \\ B_{\omega\ell m}^{\text{up}} e^{i\omega r_*}, & r_* \rightarrow \infty. \end{cases} \quad (12)$$

In the above equation, we have written the radial function $R_{s\omega\ell m}$ as a function of the “tortoise” co-ordinate r_* , which is defined in terms of the co-ordinate r by

$$\frac{dr_*}{dr} = \frac{r^2 + a^2}{\Delta_n} \quad (13)$$

for the metrics (5, 9), where Δ_n is given by (6). The frequency of the mode as seen by an observer far from the black hole is ω , but due to the rotation of the black hole an observer near the event horizon sees a modified frequency

$$\tilde{\omega} = \omega - m\Omega_H, \quad (14)$$

where Ω_H is the angular velocity of the event horizon (8). In (12), $A_{\omega\ell m}^{\text{up}}$ and $B_{\omega\ell m}^{\text{up}}$ are complex constants for each mode. The “up” modes (12) represent waves which emanate from the event horizon of the black hole. Part of the wave (the part involving $A_{\omega\ell m}^{\text{up}}$) is reflected back down the black hole, and part of the wave (the part involving $B_{\omega\ell m}^{\text{up}}$) is transmitted out to infinity. It is the latter part which contributes to the Hawking radiation observed far from the black hole.

For each particle species, the Hawking radiation is computed by summing the contributions from each “up” mode. The differential emission rates per unit time and unit frequency ω of particles (N), energy (E) and angular momentum (J) are given by

$$\frac{d^2}{dt d\omega} \begin{pmatrix} N \\ E \\ J \end{pmatrix} = \frac{1}{2\pi} \sum_{\text{modes}} \frac{|\mathcal{A}_{s\omega\ell m}|^2}{e^{\tilde{\omega}/T_H} \mp 1} \begin{pmatrix} 1 \\ \omega \\ m \end{pmatrix} \quad (15)$$

where T_H is the Hawking temperature (10), the + sign is for fermions, the – sign for bosons, and we have integrated over all angles. The quantity $|\mathcal{A}_{s\omega\ell m}|^2$ is known as the grey-body factor. It encodes the fact that the emitted radiation is not exactly thermal, due to the interaction of the emitted quanta with the gravitational potential which surrounds the black hole. The grey-body factor corresponds to the proportion of the flux emitted near the event horizon of the black hole which tunnels through the potential barrier to reach infinity. It is computed from the “up” modes (12) as follows:

$$|\mathcal{A}_{s\omega\ell m}|^2 = 1 - \left| A_{\omega\ell m}^{\text{up}} \right|^2. \quad (16)$$

There is a considerable body of work studying the Hawking radiation in these two phases of the evolution of the black hole. For the sake of brevity, here we discuss only results for neutral, massless fields and only

give a very limited number of references. Fuller discussions and more complete lists of references can be found in the detailed reviews [1, 2]. A summary of what is known about the Hawking radiation in the spin-down and Schwarzschild phases is presented in Table 2.

Spin-down phase	Schwarzschild phase
<i>Brane emission</i> [26] scalars, fermions, gauge bosons	<i>Brane emission</i> [27] scalars, fermions, gauge bosons
<i>Bulk emission</i> [28] scalars	<i>Bulk emission</i> [27] scalars
<i>Graviton emission</i> [29] partial results only	<i>Graviton emission</i> [30, 31] complete results

Table 2: Summary of Hawking radiation results during the spin-down and Schwarzschild phases of the evolution of the black hole, for neutral massless particles only.

The radiation of Standard Model particles on the brane in both the spin-down [26] and Schwarzschild phases [27] is studied using a generalization of Teukolsky's formalism [25]. Due to the comparative simplicity of the scalar field equation (even on the higher-dimensional metric (5)) the radiation of scalar particles on the brane and in the bulk is tractable [26, 27, 28]. Teukolsky's original formalism [25] was applicable to graviton (spin-2) perturbations of four-dimensional Kerr black holes, but does not easily generalize to gravitational perturbations of higher-dimensional black holes. The formalism for dealing with gravitational perturbations of spherically symmetric higher-dimensional black holes has been developed [32], which has enabled the Hawking radiation to be studied in this case [30, 31]. However, for higher-dimensional rotating black holes, the perturbation equations are much more complicated, even for singly-rotating Myers-Perry black holes (5) [33]. Unlike the spherically symmetric case, the equations describing gravitational perturbations of Myers-Perry black holes do not separate into ordinary differential equations [33], which has rendered computing the Hawking radiation intractable to date. The exception to this is tensor-type gravitational perturbations of Myers-Perry black holes, which satisfy the separable scalar field equation. There are results for the Hawking radiation for this restricted class of gravitational perturbations [29].

A key question for experimental searches is how much of the Hawking radiation is emitted on the brane (since only radiation on the brane is observable). Due to the large number of degrees of freedom in the Standard

Model, and the democratic emission of Hawking radiation, it is expected that most radiation will be on the brane [34]. However, the number of gravitational degrees of freedom increases rapidly with increasing n (the number of extra dimensions). This means that the proportion of the Hawking radiation escaping into the bulk also increases rapidly as n increases (see Table 3), although, even in eleven space-time dimensions ($n = 7$), three-quarters of the radiation is on the brane.

	$n = 0$	$n = 1$	$n = 3$	$n = 5$	$n = 7$
scalars	6.8	4.0	3.6	3.5	2.9
fermions	83.8	78.7	72.3	68.1	53.4
gauge bosons	9.3	16.7	21.7	22.2	18.6
gravitons	0.1	0.6	2.4	7.7	25.1

Table 3: Percentages of energy emission from a non-rotating black hole into particles of spin-0, $\frac{1}{2}$, 1 and 2, assuming the Standard Model of particle physics with three families and one Higgs field on the brane and only graviton emission in the bulk. Data taken from [31].

Quantum black holes

Our focus in this brief note has been the “standard” model of microscopic black hole production and decay at the LHC, in the context of the ADD brane-world scenario. In this model, the black hole is semi-classical: the metric is classical and described by general relativity, and the black hole emits quantum Hawking radiation. This semi-classical approximation breaks down when the black hole energy is roughly E_* , the energy scale at which the details of the unknown theory of quantum gravity become important. Meade and Randall [16] have argued that, in order for the black hole to be described by a classical metric, it must be the case that the Compton wavelengths of the colliding particles lie within the event horizon of the formed black hole. This implies that the black hole energy should be at least an order of magnitude larger than E_* for the semi-classical approximation to be valid.

In the absence of a full theory of quantum gravity, there have been attempts in the literature to study fully quantum black holes with energies close to E_* [18, 35], as well to refine the semi-classical picture to incorporate quantum gravity effects [36]. Fully quantum black holes do not decay thermally, but instead emit just a few particles. Particle physics symmetries are used to constrain the decay processes.

Experimental searches

There are a number of event generators simulating black hole processes at the LHC [37, 38, 39, 40]. The LHC experimental groups use CHARYBDIS2 [37] and BlackMax [38] for simulating semi-classical black holes and QBH [40] for the simulation of quantum black holes. Black hole events typically have high primary particle multiplicity with large missing transverse momentum.

At the time of writing no evidence for either semi-classical or quantum black holes has been observed at the LHC [41, 42]. These null results have enabled the LHC experimental groups to set lower bounds on the higher-dimensional quantum gravity scale E_* . ATLAS rule out semi-classical black holes having masses lower than about $4 \text{ TeV}/c^2$ for six extra dimensions and E_* about 2 TeV [41], while CMS have slightly higher lower bounds on the semi-classical black hole mass for the same values of E_* [42]. CMS also rule out quantum black holes with masses lower than about $5 - 6 \text{ TeV}/c^2$ for $E_* = 2 - 5 \text{ TeV}$ [42].

Conclusions

We have briefly reviewed the ADD large extra dimensions scenario, in which the energy scale of quantum gravity, E_* , may be as low as a few TeV. This raises the exciting possibility of probing quantum gravity effects at the LHC. Of the many possible strong gravity processes, those involving microscopic black holes will be some of the most spectacular. Our focus in this note has been a semi-classical model of microscopic black hole production and decay, with the geometry described by general relativity and quantum Hawking radiation being emitted from the black hole. We have also discussed the validity of this model and recent work on describing fully quantum black holes. To date, there has been no experimental evidence for black holes at the LHC. However, this does not diminish the importance of searching for them: the non-observation results have set lower bounds on the energy scale E_* , constraining the elusive theory of quantum gravity.

Acknowledgements

EW thanks the organizers of TAM 2013 for a very enjoyable and stimulating conference in one of the most beautiful cities in the world. She also thanks her collaborators on work relevant to this talk: Marc Casals, Sam Dolan, Gavin Duffy,

Chris Harris, Panagiota Kanti and Piero Nicolini. This work is supported by the Lancaster-Manchester-Sheffield Consortium for Fundamental Physics under STFC Grant No. ST/J000418/1 and by EU COST Action MP0905 “Black Holes in a Violent Universe”.

References

- [1] A. Casanova and E. Spallucci, *Class. Quantum Grav.* **23** (2006) R45; M. Cavaglià, *Int. J. Mod. Phys. A* **19** (2003) 1843; S. Hossenfelder, in *Focus on black hole research*, ed. P.V. Kreitler, pp. 155–192 (Nova Science Publishers, 2005); P. Kanti, *Lect. Notes Phys.* **769** (2009) 387; P. Kanti, *Rom. J. Phys.* **57** (2012) 879; G. Landsberg, *Eur. Phys. J. C* **33** (2004) S927; A.S. Majumdar and N. Mukherjee, *Int. J. Mod. Phys. D* **14** (2005) 1095; S.C. Park, *Prog. Part. Nucl. Phys.* **67** (2012) 617; B. Webber, *hep-ph/0511128*; E. Winstanley, *arXiv:0708.2656*.
- [2] P. Kanti, *Int. J. Mod. Phys. A* **19** (2004) 4899.
- [3] I. Antoniadis, N. Arkani-Hamed, S. Dimopoulos and G.R. Dvali, *Phys. Lett. B* **436** (1998) 257; N. Arkani-Hamed, S. Dimopoulos and G.R. Dvali, *Phys. Rev. D* **59** (1999) 086004.
- [4] T. Banks and W. Fischler, *hep-th/9906038*.
- [5] S. Dimopoulos and G. Landsberg, *Phys. Rev. Lett.* **87** (2001) 161602.
- [6] S.B. Giddings and S. Thomas, *Phys. Rev. D* **65** (2002) 056010.
- [7] K.S. Thorne, in *Magic without magic: John Archibald Wheeler. A collection of essays in honor of his sixtieth birthday*, ed. J. Klauder (W.H. Freeman, San Francisco, 1972).
- [8] D. Ida and K.-i. Nakao, *Phys. Rev. D* **66** (2002) 064026; C.m. Yoo, H. Ishihara, M. Kimura and S. Tanzawa, *Phys. Rev. D* **81** (2010) 024020.
- [9] P.C. Aichelburg and R.U. Sexl, *Gen. Rel. Grav.* **2** (1971) 303.
- [10] D.M. Eardley and S.B. Giddings, *Phys. Rev. D* **66** (2002) 044011.
- [11] P.D. D’Eath, *Black holes: gravitational interactions*, (Oxford Science Publications 1996).
- [12] H. Yoshino and V.S. Rychkov, *Phys. Rev. D* **71** (2005) 104028 [Erratum-ibid. *D* **77** (2008) 089905].
- [13] F. S. Coelho, C. Herdeiro and M. O. P. Sampaio, *Phys. Rev. Lett.* **108** (2012) 181102; C. Herdeiro, M. O. P. Sampaio and C. Rebelo, *JHEP* **1107** (2011) 121; M.O.P. Sampaio, *arXiv:1306.0903*.
- [14] M.W. Choptuik and F. Pretorius, *Phys. Rev. Lett.* **104** (2010) 111101; W.E. East and F. Pretorius, *Phys. Rev. Lett.* **110** (2013) 101101; L. Rezzolla and K. Takami, *Class. Quant. Grav.* **30** (2013) 012001; M. Shibata, H. Okawa and T. Yamamoto, *Phys. Rev. D* **78** (2008) 101501; U. Sperhake, V. Cardoso, F. Pretorius, E. Berti and J.A. Gonzalez, *Phys. Rev. Lett.* **101** (2008) 161101.
- [15] U. Sperhake, *Int. J. Mod. Phys. D* **22** (2013) 1330005; H.M.S. Yoshino and M. Shibata, *Prog. Theor. Phys. Suppl.* **189** (2011) 269; H.M.S. Yoshino and M. Shibata, *Prog. Theor. Phys. Suppl.* **190** (2011) 282.
- [16] P. Meade and L. Randall, *JHEP* **0805** (2008) 003.
- [17] U. Sperhake, E. Berti, V. Cardoso and F. Pretorius, *arXiv:1211.6114*.
- [18] X. Calmet, W. Gong and S.D.H. Hsu, *Phys. Lett. B* **668** (2008) 20; D.M. Gingrich, *J. Phys. G* **37** (2010) 105008.

- [19] M. Zilhao, V. Cardoso, C. Herdeiro, L. Lehner and U. Sperhake, *Phys. Rev. D* **85** (2012) 124062.
- [20] M.O.P. Sampaio, *JHEP* **0910** (2009) 008.
- [21] R. Emparan and H.S. Reall, *Living Rev. Rel.* **11** (2008) 6; S. Tomizawa and H. Ishihara, *Prog. Theor. Phys. Suppl.* **189** (2011) 7.
- [22] R. Gregory, *Lect. Notes Phys.* **769** (2009) 259; P. Kanti, *J. Phys. Conf. Ser.* **189** (2009) 012020; N. Tanahashi and T. Tanaka, *Prog. Theor. Phys. Suppl.* **189** (2011) 227.
- [23] R.C. Myers and M.J. Perry, *Annals Phys.* **172** (1986) 304.
- [24] S.W. Hawking, *Commun. Math. Phys.* **43** (1975) 199.
- [25] S.A. Teukolsky, *Phys. Rev. Lett.* **29** (1972) 1114; S.A. Teukolsky, *Astrophys. J.* **185** (1973) 635.
- [26] M. Casals, S.R. Dolan, P. Kanti and E. Winstanley, *JHEP* **0703** (2007) 019; M. Casals, P. Kanti and E. Winstanley, *JHEP* **0602** (2006) 051; G. Duffy, C. Harris, P. Kanti and E. Winstanley, *JHEP* **0509** (2005) 049; D. Ida, K.-y. Oda and S.C. Park, *Phys. Rev. D* **67** (2003) 064025 [Erratum-ibid. *D* **69** (2004) 049901].
- [27] C.M. Harris and P. Kanti, *JHEP* **0310** (2003) 014.
- [28] M. Casals, S.R. Dolan, P. Kanti and E. Winstanley, *JHEP* **0806** (2008) 071.
- [29] J. Doukas, H.T. Cho, A.S. Cornell and W. Naylor, *Phys. Rev. D* **80** (2009) 045021; P. Kanti, H. Kodama, R.A. Konoplya, N. Pappas and A. Zhidenko, *Phys. Rev. D* **80** (2009) 084016.
- [30] A.S. Cornell, W. Naylor and M. Sasaki, *JHEP* **0602** (2006) 012; S. Creek, O. Efthimiou, P. Kanti and K. Tamvakis, *Phys. Lett. B* **635** (2006) 39; D.K. Park, *Phys. Lett. B* **638** (2006) 246.
- [31] V. Cardoso, M. Cavaglià and L. Gualtieri, *JHEP* **0602** (2006) 021.
- [32] H. Kodama and A. Ishibashi, *Prog. Theor. Phys.* **110** (2003) 701.
- [33] M. Durkee and H.S. Reall, *Class. Quant. Grav.* **28** (2011) 035011; K. Murata, *Prog. Theor. Phys. Suppl.* **189** (2011) 210; H.S. Reall, *Int. J. Mod. Phys. D* **21** (2012) 1230001.
- [34] R. Emparan, G.T. Horowitz and R.C. Myers, *Phys. Rev. Lett.* **85** (2000) 499.
- [35] X. Calmet, D. Fragkakis and N. Gausmann, chapter 8 in *Black holes: evolution, theory and thermodynamics*, ed. A.J. Bauer and D.G. Eifel (Nova Science Publishers, 2012); X. Calmet and N. Gausmann, *Int. J. Mod. Phys. A* **28** (2013) 135004.
- [36] P. Nicolini and E. Winstanley, *JHEP* **1111** (2011) 075.
- [37] J.A. Frost, J.R. Gaunt, M.O.P. Sampaio, M. Casals, S.R. Dolan, M.A. Parker and B.R. Webber, *JHEP* **0910** (2009) 014.
- [38] D.-C. Dai, G. Starkman, D. Stojkovic, C. Issever, E. Rizvi and J. Tseng, *Phys. Rev. D* **77** (2008) 076007.
- [39] M. Cavaglià, R. Godang, L. Cremaldi and D. Summers, *Comput. Phys. Commun.* **177** (2007) 506; D.M. Gingrich, [hep-ph/0610219](https://arxiv.org/abs/hep-ph/0610219); G.L. Landsberg, *J. Phys. G* **32** (2006) R337.
- [40] D.M. Gingrich, *Comput. Phys. Commun.* **181** (2010) 1917.
- [41] G. Aad *et al.* [ATLAS Collaboration], *Phys. Lett. B* **716** (2012) 122.
- [42] S. Chatrchyan *et al.* [CMS Collaboration], [arXiv:1303.5338](https://arxiv.org/abs/1303.5338).